

# Grafting Methacrylic Acid onto Carboxymethyl Tamarind Kernel Polysaccharide to Improve pH Sustained Release Responsive Hydrogel Matrix

A. DAS, K. MUKHERJEE AND T. K. GIRI\*

Department of Pharmaceutical Technology, Jadavpur University, Kolkata, West Bengal 700032, India

## Das *et al.*: pH Responsive Sustained Release Hydrogel Matrix

The grafting of carboxymethyl tamarind polysaccharide with methacrylic acid was done by using ammonium persulfate as an initiator. The grafting reaction was done by a conventional method. The grafted copolymer and the native polymer were then used to prepare matrix tablets loaded with ibuprofen for the pH-dependent release of ibuprofen in the intestinal region. The effect of grafting reaction conditions on percentage grafting and percentage grafting efficiency was studied. Fourier transform infrared spectroscopy confirmed the grafting reaction. X-ray diffraction and differential scanning calorimetry studies indicated that ibuprofen crystallinity was maintained in the matrix formulations. The important finding of the investigation was that the matrix tablets provided pH-dependent sustained ibuprofen release in the intestinal pH which would bypass the problems associated with ibuprofen administration and thereby enhance patient acceptability and compliance. The matrix tablets released <8 % of the loaded ibuprofen in the gastric pH and provided sustained ibuprofen release in intestinal pH. Future directions should perform the *in vivo* pharmacokinetic and pharmacodynamic studies. It can be concluded that the developed hydrogel matrix tablets could be used to prevent gastric disorders associated with ibuprofen and enhance patient compliance by reducing the dosing frequency.

**Key words:** Ibuprofen, carboxymethyl tamarind polysaccharide, pH-dependent sustained release, matrix tablets, grafting

Over the last decade, demand for polysaccharides has increased significantly in pharmaceutical and biomedical fields. Polysaccharides can be obtained from plants (tara gum), animals (hyaluronic acid), bacteria (gellan gum) and fungi (pullulan)<sup>[1-4]</sup>. In biomedical fields, they are used in tissue engineering, biosensors and bio imaging fields<sup>[5]</sup>. In pharmaceutical fields, they are used for targeted and sustained drug delivery<sup>[6,7]</sup>. Polysaccharides are also used for the development of matrix tablets, bilayer tablets, hydrogel tablets and hydrogel beads<sup>[8-11]</sup>. These polysaccharides are non-toxic, cheap, biocompatible and biodegradable<sup>[12,13]</sup>. Moreover, their polymeric chains and numerous functional groups are acquiescent to diverse modifications and derivatizations. However, these polysaccharides have certain drawbacks. These limitations include batch-to-batch variability, limited mechanical strength and environmental sensitivity, low stability, poor solubility and limitation of control drug release and degradation in the biological fluid.

Several strategies such as physical modification (crosslinking), polymer blending and mixing, and graft polymerization techniques are used to bypass the limitations that pose problems in preparing polysaccharide-based drug delivery systems. It can also be modified chemically through carboxy methylation, hydroxylation and thiolation. Among the various approaches, grafting appeared as a potential option that can be used to resolve the natural polysaccharide's limitations in drug delivery systems and maximize their efficacy and safety<sup>[14,15]</sup>. Graft polymerization involves the covalent attachment of synthetic polymers onto the other polysaccharide backbone, resulting in hybrid materials with properties of either polymer<sup>[16]</sup>. Grafting the backbone

This is an open access article distributed under the terms of the Creative Commons Attribution-NonCommercial-ShareAlike 3.0 License, which allows others to remix, tweak, and build upon the work non-commercially, as long as the author is credited and the new creations are licensed under the identical terms

Accepted 27 September 2024

Revised 17 May 2024

Received 10 June 2023

Indian J Pharm Sci 2024;86(5):1702-1716

\*Address for correspondence

E-mail: tapan\_ju01@rediffmail

of cellulose, dextrin, starch, chitosan and guar gum with various vinyl monomers has been done<sup>[17-21]</sup>. Graft procedures provided improved stability and solubility, reducing toxicity, bioavailability, targeted drug release, and biocompatibility<sup>[22,23]</sup>. Grafting can also improve the sustained release property of the delivery system. A study showed that grafting poly(N-isopropyl acrylamide) onto cellulose nanofibers could provide control drug release due to temperature-responsive behavior of the matrix. Grafting also provided sustained drug release at the target location temperature<sup>[24]</sup>. Hydrogels based on polyacrylamide grafted sodium alginate provided sustained famotidine (an anti-ulcer drug) release for up to 12 h providing gastro-protective/retentive properties<sup>[25]</sup>. The chitosan was grafted with acrylic acid and acrylamide for the controlled release of protein. Sustained release of the protein from the prepared grafted hydrogel at pH 6.8 and 7.4 were observed<sup>[26]</sup>. Polyacrylamide-grafted carboxymethyl guar gum had improved sustained release properties than the carboxymethyl guar gum<sup>[27]</sup>. Previous literature indicated the potential of grafting procedures in improving drug delivery systems. Grafting of natural polysaccharides can also be used to provide pH responsive drug release, where the drug will be released in response to a specific pH. The pH responsive drug release can be beneficial for modulating the site of drug release and also to protect the drug/bioactive from the various degrading factors of the gastrointestinal tract.

Ibuprofen (IBU), a Nonsteroidal Anti-Inflammatory Drugs (NSAIDs), is prescribed for the palliative management of rheumatoid arthritis, ankylosing spondylitis and osteoarthritis. The biological half-life ( $t_{1/2}$ ) of IBU is around 2.2 h and is thus administered frequently to maintain steady plasma concentration. However, long-term use of NSAIDs produces slight gastric irritation to severe bleeding, ulceration and gastric mucosa perforation. All these factors lead to patient non-compliance and discomfort<sup>[28]</sup>.

Herein this research article aimed to develop Methacrylic Acid (MAA) grafted Carboxymethyl Tamarind Polysaccharide (CMTKP) matrix tablets for sustained IBU delivery. The objective is to provide pH-dependent IBU release from the matrix tablets, where there will be minimum IBU release in the gastric mucosa and sustained release in the intestinal region. This release profile will not only minimize the gastric side effects of IBU but will also minimize the dosing frequency which will promote

patient compliance and reduce the cost of treatment. Confirmation of the grafting was done through Fourier Transforms Infrared (FTIR) analysis. The compatibility of IBU in the matrix tablets and the mechanism of IBU release from the matrix tablets were also studied. The limitation of the work was handling MAA which has low boiling point and was unable to use in the grafting process by conventional microwave method and also higher temperature.

## MATERIALS AND METHODS

### Materials:

IBU was brought as a gift from Industrial Organics Ltd., Chemicals, Mumbai, India. CMTKP was gifted by Hindustan Gum and Chemical Ltd., Bhiwani, India. MAA and Ammonium Persulfate (APS) were procured commercially from Merck, Mumbai, India.

### Synthesis of MAA acid grafted CMTKP:

CMTKP (0.3-0.45) g was added to distilled water (30 ml) and allowed to swell overnight for complete hydration. It was then transferred to a three-necked round-bottom flask and stirred in a temperature-controlled water bath<sup>[29]</sup>. When the polymer dissolved completely in the solvent, continuous bubbling of nitrogen gas was done to maintain an inert atmosphere. To complete the grafting reaction, the process was continued for 1-2.5 h at 40°-60°. Also, an initiator, APS (10-30) mM was added to the mixture under continuous stirring conditions. MAA (0.06-0.08) mol, the monomer, was added and the reaction continued for the specified time. Then the product was taken out and cooled to terminate the reaction and then precipitated in acetone.

### Purification procedure of the synthesized grafted copolymer:

The unreacted MAA, CMTKP and their homo polymers produced during the grafting polymerization reaction must be removed to get the pure MAA grafted CMTKP (CMTKP-g-MAA). The grafted polymer was precipitated in acetone as it was insoluble in it. The homo Polymer of MAA (PMAA) is soluble in water, methanol and its mixture. The synthesized polymer was washed with a methanol and water mixture (80:20) to remove the homo polymer. Then, the grafted copolymers were first air-dried and then oven-dried to constant weight. The dried grafted copolymer is then crushed and strained through a #52 BS sieve. The grafting criteria were determined.

$$\text{Percentage Grafting (\% G)} = \frac{W_1 - W_0}{W_0} \times 100 \quad (1)$$

$$\% G = \text{Efficiency (\% GE)} = \frac{W_1 - W_0}{W_2} \times 100 - \frac{W_0}{W_2} \times 100 \quad (2)$$

Where,  $W_1$ =graft copolymer weight;  $W_0$ =polysaccharide weight and  $W_2$ =monomer weight

#### FTIR analysis:

FTIR spectra (4000-400)  $\text{cm}^{-1}$  of CMTKP, MAA and CMTKP-g-MAA were recorded in an FTIR spectrophotometer (Alpha E, Bruker, United States of America (USA)). The samples were blended with Potassium bromide (KBr) and transformed into pellets in a hydraulic press.

#### Preparation of matrix tablets:

CMTKP-g-MAA and IBU were blended and moistened with isopropyl alcohol to form a coherent mass and passed through the 18 mesh screen (Table 1). The granules were dried to constant weight and passed through 22 mesh screens. Then the granules were mixed with magnesium stearate and compressed into tablets using a tablet machine (RIMEK, Karnavati Engineering, Ltd., Gujarat, India).

#### Differential Scanning Calorimetry (DSC) study:

DSC thermograms of pure IBU and IBU-loaded tablets were obtained using DSC (Perkin Elmer DSC, STA 8000, USA). The study specifications are  $30^\circ$ - $300^\circ$ ,  $10^\circ/\text{min}$  and 20 ml/min nitrogen flow.

#### X-Ray Diffraction (XRD) study:

XRD patterns of IBU and IBU-loaded tablets were created using an X-ray diffractometer (Bruker axs, D8 Advance, USA) at a 40 kV voltage,  $25^\circ$  and 40 mA current. The samples were fixed on a holder and were scanned at 0.5 s speed with the  $5^\circ$ - $50^\circ$  diffraction angle ( $2\theta$ ) range.

#### Determination of drug content:

A matrix tablet was grounded in a mortar pestle and a

sample corresponding to 3 mg of IBU was added to 100 ml pH 7.4 buffer media and shaken. The drug solution was filtered and aliquot analyzed at 223 nm using an Ultraviolet (UV)-visible spectrophotometer (UV-2450, Shimadzu, Japan).

#### Physical characterization of table:

IBU matrix tablets were examined for thickness, friability, weight variation and hardness.

**Weight variation:** The weight of 20 tablets was taken in an electronic balance. The average was calculated and the Standard Deviation (SD) was measured.

**Thickness:** 10 randomly chosen tablets were measured for thickness with a digimatic slide caliper. Data are presented as mean $\pm$ SD, n=10.

**Friability:** 6 tablets from each batch were weighed and introduced in a friabilator (Roche Friabilator, Veego, Mumbai, India). The tablets were subsequently dedusted, gathered and weighed again. The percentage of weight loss determined the degree of friability.

#### Swelling study:

Swelling of matrix tablets was done in the United States Pharmacopeia (USP)-II dissolution apparatus (Total Distribution Points (TDP)-06P TDP-06P, Electro Lab, Mumbai, India) considering the pH values and transit time prevailing in various segments of the gastrointestinal tract. The swelling study was conducted in an acidic solution of pH 1.2 for 2 h and then in a buffer solution of pH 7.4 for up to 8 h. A weighted matrix tablet was placed in a mesh basket. The basket was then put in a vessel containing a test medium and stirred at 75 revolutions per minute (rpm). The wet matrix tablet was removed, blotted and again weighed at predetermined intervals. The swelling ratio was then calculated using the below mentioned equation

**TABLE 1: COMPOSITION OF MATRIX TABLETS**

Formulation code	Amount of CMTKP (mg)	Amount of grafted CMTKP (mg)	Ratio between CMTKP: CMTKP-g-MAA	Amount of drug (IBU)	Amount of magnesium stearate (mg)
F1	175	25	1:0.15	100	1
F2	150	50	1:0.3	100	1
F3	100	100	1:1	100	1
F4	50	150	1:3	100	1
F5	25	175	1:6	100	1
F6	200	0	1:0	100	1

$$\text{Swelling ratio \%} = \frac{W_w - W_i}{W_i} \times 100 \quad (3)$$

Where,  $W_i$ =initial matrix tablet weight and  $W_w$ =weight of tablet after time t

### Erosion study:

The erosion study was conducted using a similar methodology to the swelling experiment. At definite time intervals of 0.5 h, 1 h, 2 h, 3 h, 4 h, 5 h, 6 h, 7 h and 8 h the wet matrix tablet was taken out from the test media and dried to a constant weight at 70° and again weighed. The erosion percentage at different times was calculated using the following equation.

$$\% \text{ erosion} = \frac{W_i - W_d}{W_i} \times 100 \quad (4)$$

Where,  $W_i$ =initial weight of the tablet and  $W_d$ =dry weight of the tablet at time t.

### In vitro drug release study:

*In vitro* IBU release was performed in the dissolution apparatus (TDP-06P, Electro Lab, Mumbai, India) at 37°±0.5° and 75 rpm as per Indian Pharmacopoeia (IP) 2010. A matrix tablet was submerged for 2 h in a 700 ml of Hydrochloric acid (HCl) buffer (pH 1.2). After that, tri-sodium orthophosphate dodecahydrate (0.2 M, 200 ml) was added to the dissolution medium to raise the pH to 7.4 and the IBU release was continued to 8 h in a 900 ml pH 7.4 phosphate buffer solution. At specified time intervals, a 10 ml aliquot was withdrawn and replaced with a buffer solution. The absorbance was measured at 221 nm for the acid solution and 223 nm for the pH 7.4 phosphate buffer solution using a spectrophotometer and the amount of IBU released was measured.

### Diffusion Coefficient (DC) of the drug:

DC of IBU from the matrix tablets was determined as stated below. The equivalent spherical diameter (cm) of the tablets was determined.

$$d = (6r_c h)^{1/3} \quad (5)$$

Where, d,  $r_c$  and h represent equivalent spherical diameter, radius and height (cm) of the tablets, respectively.

DC (cm<sup>2</sup>/s) were determined using the below-mentioned equation<sup>[30]</sup>

$$DC = \pi \times (r\theta/6M_\infty)^2 \quad (6)$$

Where, r=equivalent spherical radius;  $\theta$ =slope of the straight line of  $M_t/M_\infty$  vs. the  $t_{1/2}$  plot;  $M_t$ =IBU released at time t (s) (mg) and  $M_\infty$ =total IBU loaded in matrix

tablet (mg).

### Drug release mechanism:

The drug release (up to 60 %) from the matrix tablet fitted to the power law<sup>[31]</sup>. The power law equation was developed to define the mechanism of drug release from swellable matrices. The matrix could be a sphere, cylinder and sheet. Based on the geometrical shape of the matrix, n values are defined and n values are different for different geometries. When there will be 60 % drug release from the matrix (which can either be a sphere or cylinder, etc.), pores and channels will be developed throughout the matrix. This will affect the geometry of the matrix and the matrix will not be defined by any specific geometrical shape. This will affect the n values and proper prediction of the drug release mechanism will not be done. Thus to avoid any ambiguity, drug release only up to 60 % is taken into account.

$$M_t/M_\infty = kt^n \quad (7)$$

Where,  $M_t$ =drug released at time t;  $M_\infty$ =drug released at equilibrium; K=constant and n=diffusional exponent.

In the case of the cylindrical matrix such as a tablet, 0.45 indicated Fickian diffusion and 0.45<n<0.89 indicates anomalous transport.

### Statistical analysis:

Analysis of Variance (ANOVA) was done using GraphPad Prism (version 3.0) to determine the statistical significance of the data generated from swelling, erosion and drug release studies. The difference was deemed significant when p<0.05.

## RESULTS AND DISCUSSION

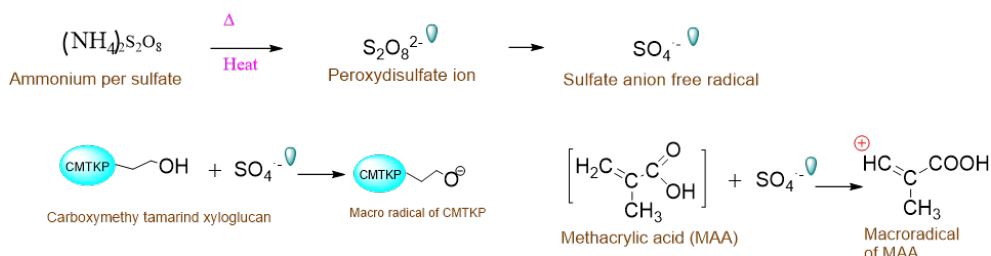
CMTKP-g-MAA was synthesized by the free radical polymerization method. The reaction process has been illustrated in fig. 1. The grafting process is facilitated when APS is employed as an oxidizing initiator because of the removal of the hydrogen atom from the CMTKP. This generates CMTKP macro radicals<sup>[32]</sup>. The monomer molecules, which are in close vicinity of reaction sites, become acceptors of CMTKP macro radicals, resulting in chain initiation and thereafter themselves become free radical donors to neighboring molecules leading to propagation. These grafted chains are ended by coupling to give graft copolymer.

The FTIR spectra of CMTKP, MAA and CMTKP-g-MAA are depicted in fig. 2. A wide absorption band in CMTKP at 3445 cm<sup>-1</sup> is because of Hydroxyl (-OH)

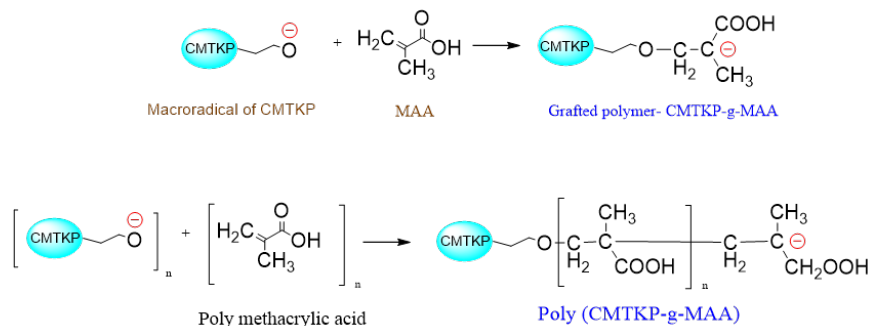
group stretching. A strong band around  $1010\text{ cm}^{-1}$  due to the primary alcohol group of CMTKP polysaccharide was noted. The dual peaks at  $1643\text{ cm}^{-1}$  and  $1415\text{ cm}^{-1}$  are the asymmetric and symmetric  $-\text{COO}-$  groups in CMTKP. The other authors have observed similar peaks<sup>[33-35]</sup>. MAA shows an absorption band at  $1637\text{ cm}^{-1}$  ( $\text{C}=\text{C}$  stretching) which is due to the vinyl unsaturation present in MMA monomer<sup>[36]</sup>. CMTKP-g-MAA shows a wide absorption band at  $3443\text{ cm}^{-1}$  due to  $-\text{OH}$  group stretching. The reduced intensity of the hydroxyl group ( $-\text{OH}$ ) absorption band between  $3600\text{ cm}^{-1}$  and  $3000$

$\text{cm}^{-1}$  confirmed that the  $-\text{OH}$  groups of CMTKP were grafted with MAA. The  $\text{C}-\text{H}$  stretching vibration band is at  $3001\text{ cm}^{-1}$ . An intense absorption band at  $1703\text{ cm}^{-1}$  confirms the  $\text{C}=\text{O}$  (carbonyl group) presence. The band at  $1637\text{ cm}^{-1}$  ( $\text{C}=\text{C}$  stretching) present in the spectrum of MAA is absent in the spectrum of the grafted polymer, indicating the homo polymerization process. This carbonyl group indicates the insertion of MAA onto the CMTKP backbone. The other authors have observed similar peaks in MAA grafted chitosan<sup>[37]</sup>.

### Initiation



### Propagation



### Termination

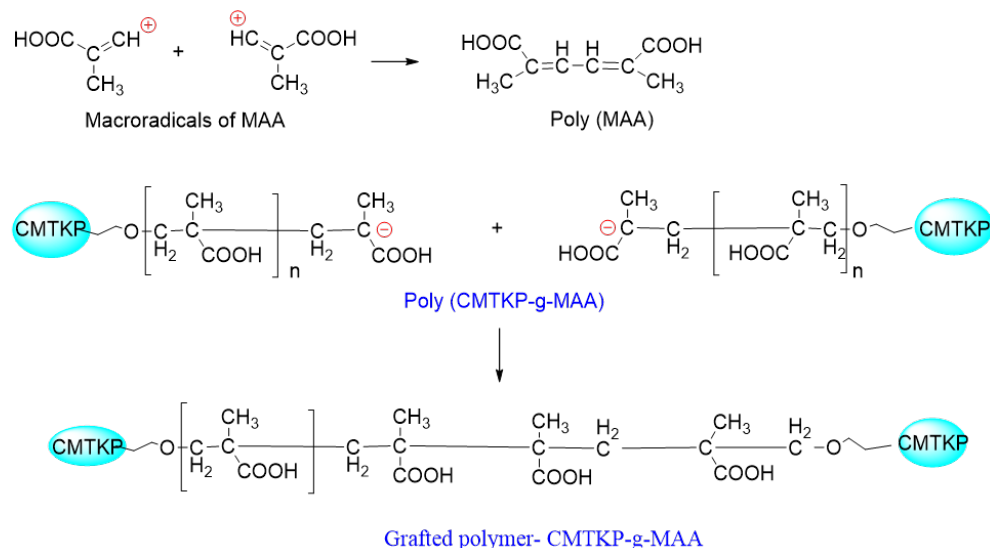
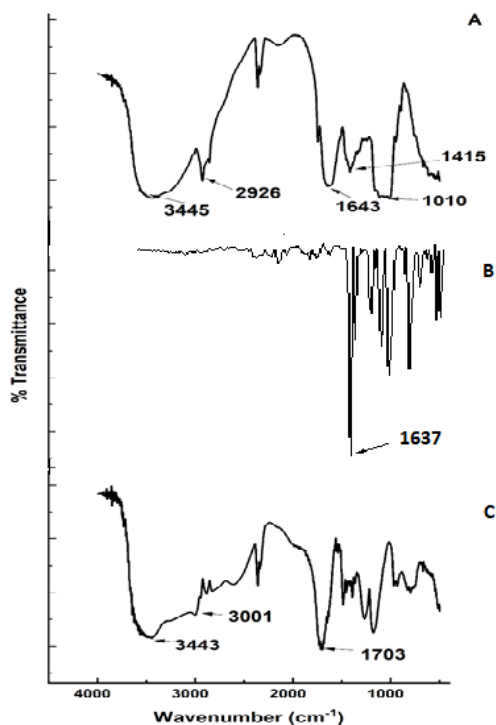


Fig. 1: Schematic representation of the mechanism of graft co-polymerization



**Fig. 2:** FTIR spectra, (A): CMTKP; (B): MAA monomer and (C): CMTKP-g-MAA

The optimum grafting condition was achieved by altering the concentration of monomer, initiator and polysaccharide along with grafting temperature and time. Fig. 3 illustrates the effect of grafting reaction time on MAA graft copolymerization onto CMTKP backbones. Reaction time varied from 1-2.5 h. The more the time of exposure of monomer molecules with the CMTKP macro radicals, the greater was % GE and % G. The % GE and % G at 1 h were 10 % and 155 % respectively. At the end of 2.5 h, it was 441 % and 28 %. Beyond 2.5 h, it was impossible to carry out the reaction as the product became a hard gel mass. It may be possible that after 2.5 h of the grafting reaction, the water present in the system has evaporated, which made the mass turn into a hard gel. Since the mass turned into a hard gel, mutual diffusion of the reactants (initiator, monomer and polysaccharide chains) was hindered. This resulted a decrease in the % GE and % G. The other authors have observed similar observations in MAA grafted guar gum<sup>[38]</sup>.

The effect of grafting temperature on % G and % GE was noted at temperatures 40°, 50° and 60° (fig. 4). The % G and % GE were 0 % at 40° then increased to 826 % and 53 % with an increase in temperature at 50° and then declined to 441 % and 28 % at 60°. The initial increase in % G and % GE was because of the higher diffusion of MAA molecules to macro radicals. Additionally, at elevated temperatures the solubility of the reactants

increases, thereby increasing the grafting reaction rate. As the temperature of a solution is increased, the average kinetic energy of the molecules that make up the solution also increases. This increase in kinetic energy allows the solvent molecules to break apart the solute molecules that are held together by intermolecular attractions. At increased temperatures, there may be higher molecular collisions between CMTKP and APS leading to an increase in CMTKP macro radicals. This increases graft polymerization. The fall in % GE and % G at 60° is due to a considerable rise in the rate of chain transfer between grafted chains and monomer molecules themselves and leads to chain termination reactions. Additionally above 50°, it may be possible that some of the monomer, MAA is volatilized out. The other authors have observed similar observations<sup>[39]</sup>.

Keeping other reaction conditions constant, graft copolymerization was studied at different APS concentrations. The % G and % GE increase with increasing the initiator concentration (fig. 5). It may be due to increased macro radical formation. Moreover, at higher APS concentrations, more APS free radicals attack the saccharide unit of CMTKP and reach a maximum value (% GE=53.74 and % G=826) at 20 mm. Further increase of concentration of APS beyond 20 mm disfavored the grafting reaction. The increased CMTKP macro radicals may get terminated before MAA is attached to the active site in a higher

concentration of APS. So the relatively high APS concentration caused the reduction of % G and % GE. Additionally, a drop in the % GE and % G (% GE=24 % and % G=38 %) could result from homo polymer generation at greater APS concentrations. The generated homo polymer competes with the grafting reaction

for available monomers. Oxidative degeneration of polysaccharide carbon chains by excessive free radicals may be the other likely reason for the reduced grafting at higher APS concentrations. The other authors have observed similar oxidative degradation in chitosan in the presence of potassium persulfate<sup>[40]</sup>.

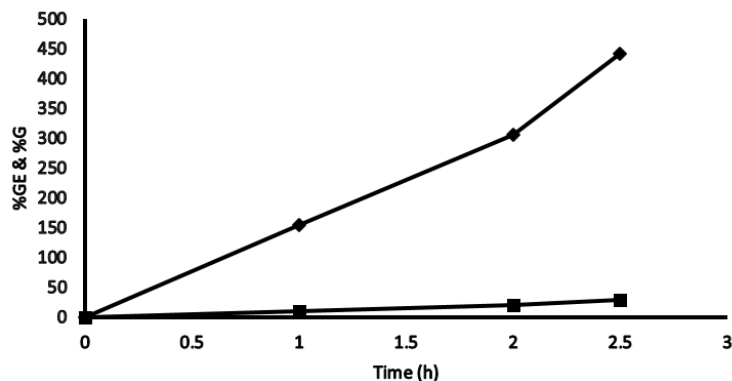


Fig. 3: Effect of grafting reaction time on MAA graft copolymerization onto CMTKP backbones  
Note: (■): % GE and (◆): % G

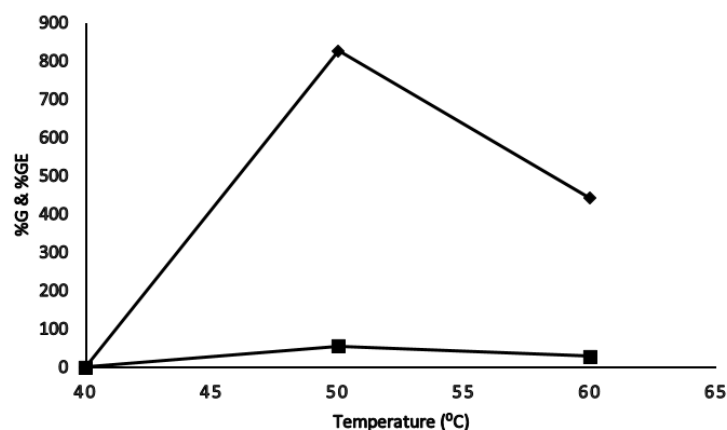


Fig. 4: Effect of temperature on grafting parameters  
Note: (■): % GE and (◆): % G

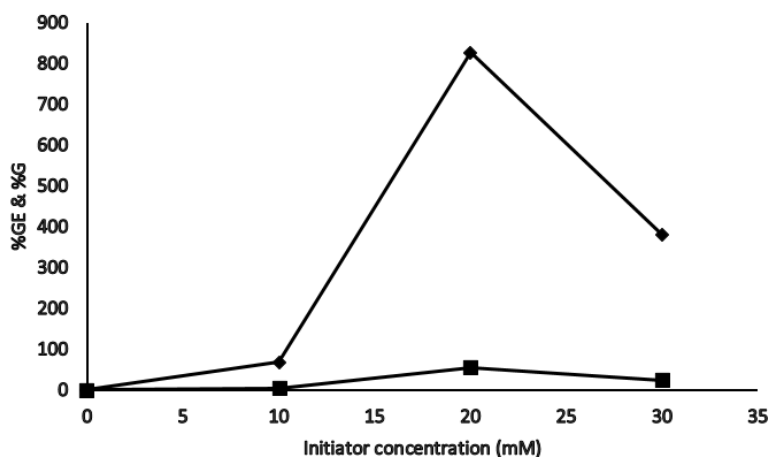


Fig. 5: Increase in % G and % GE with initiator concentration  
Note: (■): % GE and (◆): % G

When the concentration of MAA was increased from 0.08-0.1 mol, there was an initial increase in both % G and % GE (fig. 6). At 0.1 mol of monomer the optimum values for % GE (66 %) and % G (1248 %) were obtained. The initial increase in % G and % GE was because of the greater availability of monomer molecules near CMTKP macro radicals. However, beyond 0.1 mol, % G and % GE decreased because of the generation of a greater percentage of the homo polymer of MAA in the growing grafted chain. A homo polymer is the repeating unit of a monomer. The formation of homo polymer irreversibly inhibits grafting co-polymerization by reducing the availability of the monomer molecules, which are supposed to be introduced in the polysaccharide backbone. CMTKP reaction sites remained the same though the concentration of MAA was increasing and MAA homo polymer chains growing. The other authors have observed similar observations<sup>[41]</sup>.

Fig. 7 shows the effect of CMTKP concentration on the grafting parameters. As the amount of CMTKP is increased, more grafting sites are created, which are advantageous for grafting. This explains the initial increase in grafting parameters that accounts for up to 1.5 % of the CMTKP value. Beyond that, % GE and % G declined, perhaps owing to an increased viscosity

which hindered the process in the reaction medium. At higher viscosity of the reaction medium, the diffusion of the monomer, initiator and polysaccharide chains are hindered, which slows down the grafting reaction. The other authors have observed similar observations<sup>[42]</sup>.

The physical properties of the IBU matrix tablets are shown in Table 2. The friability and weight of the IBU matrix tablets were within acceptable IP limits. The amount of IBU variation from the labeled potency in each tablet was within the  $\pm 15$  % limit permitted by IP. Thus, the tablet's physical properties complied with the prescribed IP limits.

The DSC thermogram of IBU and IBU-loaded powder matrix tablets are presented in fig. 8. IBU presented a sharp melting peak at 77° and a broad decomposition endotherm at 239° corresponding to the complete decomposition or evaporation of IBU. IBU-loaded powdered matrix tablet formulation showed reduced endotherm at 77°, indicating that the degree of crystallinity of IBU decreased in the formulation. Similar observations of IBU were found in other reports. Another endotherm peak becomes broader and shifted to 229° as degradation was initiated early due to the softening of the polysaccharide chain bonds during the process of wet granulation<sup>[43]</sup>.

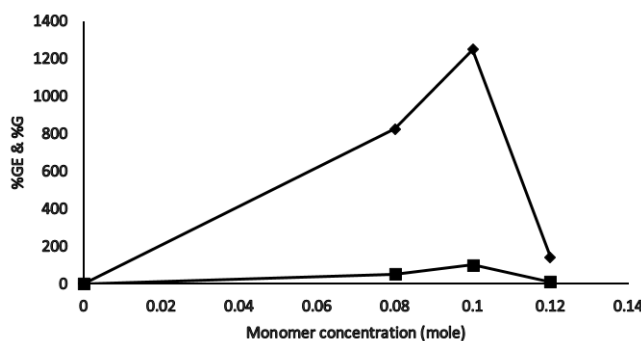


Fig. 6: Effect of monomer concentration

Note: (■): % GE and (◆): % G

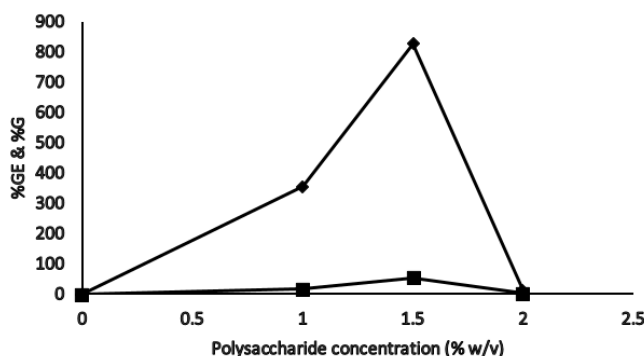


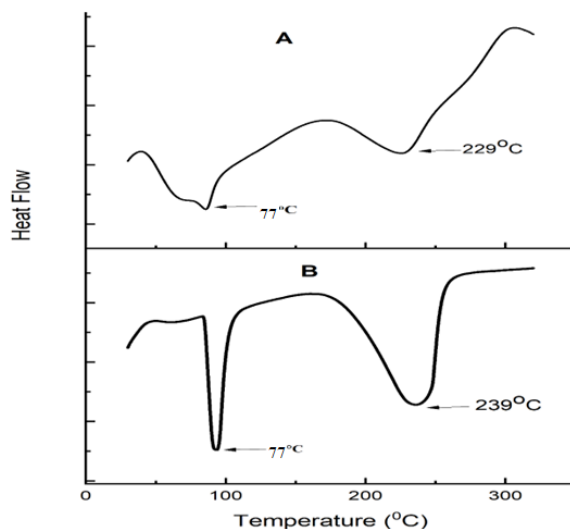
Fig. 7: Effect of CMTKP concentration on the grafting parameters

Note: (■): % GE and (◆): % G



**TABLE 2: PHYSICAL CHARACTERISTICS OF THE TABLETS**

Formulations	Weight (mg) (mean±SD, n=20)	Drug content (mg) (mean±SD, n=3)	Thickness (mm) (mean±SD, n=10)	Friability (%)
F1	300.22±1.02	86.0±1.67	3.02±0.56	0.16
F2	298.45±1.11	91.0±1.54	3.01±0.54	0.18
F3	294.02±1.34	87.2±1.77	2.93±0.81	0.2
F4	299.94±1.45	88.0±1.24	2.89±0.93	0.22
F5	301.09±1.56	101.0±0.47	3.06±0.61	0.23
F6	299.09±1.01	100.9±0.12	3.00±0.49	0.15

**Fig. 8: DSC curve, (A): IBU loaded tablet formulation and (B): IBU sample**

The XRD of IBU and drug-loaded matrix tablet are shown in fig. 9. IBU has four significant peaks with diffraction angles ( $2\theta$ ) are  $5.84^\circ$ ,  $16.34^\circ$ ,  $19.74^\circ$  and  $22^\circ$  with intensities of 9145, 6872, 8744, 13 196. Drug-loaded tablet powder formulation exhibited peaks with diffraction angles ( $2\theta$ ) are  $5.92^\circ$ ,  $16.43^\circ$ ,  $19.98^\circ$  and  $22.16^\circ$  with intensities of 2454, 3560, 3607, 2289. However, the peak intensities of IBU-loaded tablet formulation were less than that of pure drugs. Peak intensity reduction from aqueous latex of acrylate and methacrylate copolymer-coated IBU pellets was also noted<sup>[44]</sup>.

The swelling behaviour of the developed tablets was represented in fig. 10. The swelling behaviour of CMTKP and grafted CMTKP tablets depended on the medium pH. The swelling was significantly less in acidic media and higher in the basic media ( $p < 0.05$ ). Moreover, the swelling of the matrix tablets increased with the increase in the proportion of the grafted copolymer. In acidic pH 1.2, the carboxymethyl groups on the CMTKP polymer chains undergo protonation, resulting in a decrease in the negative charge on the polymer.

This reduction in charge density also helps to reduce the forces pushing negatively charged carboxylate ions away from each other which can diminish the osmotic pressure within the tablet and therefore results in less swelling. Furthermore, the swelling properties also depended on the ratio of CMTKP to CMTKP-g-MAA in the matrix<sup>[45]</sup>. When CMTKP is grafted with MAA, it forms a copolymer that may be used in tablet formulations as a pH-sensitive material. So, incorporating the minimum amount of CMTKP graft MAA (25 mg, F1) within the tablet matrix showed a slower rate of swelling in the acidic medium due to protonated carboxylic acid groups on the MAA units, resulting in a lower charge density on the copolymer. This leads to decreased swelling of the tablet. Additionally, the acidic pH can lead to the development of compact cross-links between the polymer chains, further reducing their water uptake and swelling<sup>[46]</sup>. Further, increasing the graft copolymer amount from 50 mg (F2) to 175 mg (F5) caused increased swelling due to the greater availability of carboxymethyl groups in the bulk causing repulsion leading to the relaxation

of polymeric chains in the acidic medium. In contrast, after 2 h when the acidic pH changes to basic pH 7.4, the carboxymethyl groups on the CMTKP and CMTKP grafted MAA polymer chains are deprotonated, resulting in a higher negative charge on the polymer. This increased charge density could be the reason for more swelling in the basic medium. Furthermore, the basic pH may lead to the formation of looser cross-links between the polymer chains, allowing for greater water uptake and swelling. Therefore, the difference in swelling behavior between acidic and basic pH can be attributed to the changes in charge density and cross-linking of the CMTKP polymer chains under different pH conditions. A similar kind of observation has been reported where the carboxymethyl cellulose grafted MAA swelling increased with the higher concentration of MAA's hydrophilic carboxylic groups<sup>[47]</sup>.

The erosion behavior of the developed tablets was represented in fig. 11 and Table 3. Erosion was significantly less in acidic media and higher in the basic media ( $p < 0.05$ ). Moreover, an increase in the proportion of the grafted copolymer in the matrix tablets led to a significant rise in the erosion of the matrix tablets ( $p < 0.05$ ). In acidic medium when only CMTKP is used, the rate of media penetration in the matrix tablets is higher than the erosion rate. In pH 1.2, the protonated carboxymethyl groups of the CMTKP

polymer chains decreased the negative charge on the polymer. This reduction in charge density can lead to a fall in the repulsive forces between the polymer chains and may result in tighter packing of the polymer chains. As a result, the CMTKP tablets may exhibit less erosion. Furthermore, adding low amounts of grafted polymers (25 mg, F1) in the matrix tablet also exhibits lower erosion due to protonated carboxymethyl groups of MAA chains and CMTKP. Increasing the amount of grafted polymers (up to 175 mg, F5), the penetration rate of the medium and erosion was greater due to the repulsion of carboxylate ions initiated erosion earlier. Then in the pH 7.4 basic medium, the polymers reached their maximal swelling. The deprotonated carboxymethyl groups in CMTKP and MAA in graft polymer chains resulted in a higher negative charge on the polymer. This increase in charge density can lead to a higher repulsive force between the polymer chains, causing a saggy arrangement of the polymer chains. As a result, the CMTKP tablets may exhibit more erosion. It was observed that the layer swelled up quickly as the penetration medium permeates the matrix more rapidly than the polymer's erosion rate formed with two movable boundaries. Following the penetration of the medium, that boundary line between the swollen layer and the glassy layer penetrates inward. This leaves the swollen layer behind, which erodes and bulk erosion occurs<sup>[48,49]</sup>.

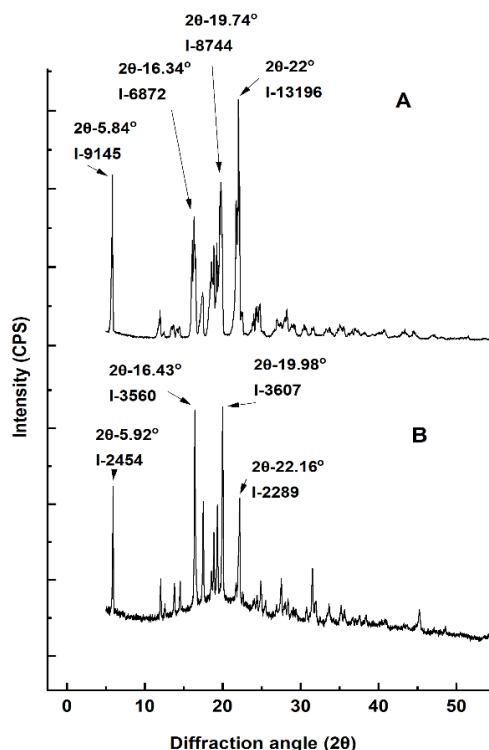


Fig. 9: XRD study, (A): IBU and (B): IBU loaded tablet powder formulation

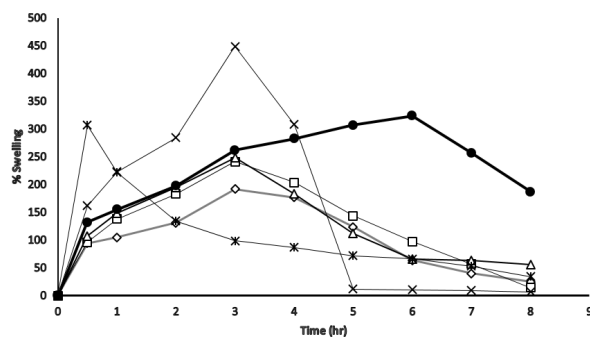


Fig. 10: Swelling study of different tablet formulations in acid media pH 1.2 for 2 h followed by basic media in pH 7.4 up to 8 h  
Note: CMTKP/CMTKP-g-MAA, (F1 $\diamond$ ): 175:25; (F2 $\square$ ): 150:50; (F3 $\triangle$ ): 100:100; (F4 $*$ ): 50:150; (F5 $\times$ ): 25:175 and (F6 $\bullet$ ): 200:0

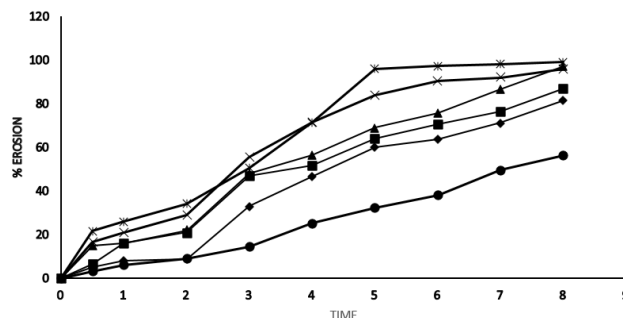


Fig. 11: Erosion study of different tablet formulations in acid media pH 1.2 for 2 h followed by basic media in pH 7.4 up to 8 h  
Note: CMTKP/CMTKP-g-MAA: (F1 $\bullet$ ): 175:25; (F2 $\blacklozenge$ ): 150:50; (F3 $\blacksquare$ ): 100:100; (F4 $\blacktriangle$ ): 50:150; (F5 $\times$ ): 25:175 and (F6 $*$ ): 200:0

TABLE 3: EROSION STUDY OF MATRIX TABLETS

Time (h)	F1	F2	F3	F4	F5	F6
0	0	0	0	0	0	0
0.5	2.9	6.5	15	16.5	21.5	3.081
1	7.897	16	16	21	26	6.188
2	7.954	21	22	29	34	9.022
3	32.996	47	48	55.5	50.5	14.562
4	46.416	51.5	56.5	71.5	71.5	25.136
5	60	64	69	84	96	32.109
6	63.787	70.5	75.5	90.5	97.391	38.204
7	71.192	76.5	86.5	95	100	49.726
8	81.518	87	97	98.5	100	56.25

The release of drugs from the matrix tablets is depicted in fig. 12. IBU release was less in acidic media and higher in the basic media. At 30 min, drug release from F1-F6 formulations was 0.182 %, 0.500 %, 2.261 %, 3.228 %, 7.132 % and 3.460 % respectively and significantly different ( $p < 0.05$ ). At 2 h, drug release from F1-F6 formulations were 1.296 %, 1.824 %, 6.495 %, 7.089 %, 14.596 % and 6.617 % respectively and significantly different ( $p < 0.05$ ). The tablet swelled and released IBU to different extents, forming a bulk matrix dependent on the polymer/grafted copolymer proportion (fig. 12).

In acidic media pH 1.2, the carboxymethyl groups on the CMTKP polymer chains can undergo protonation, resulting in a decrease in the negative charge on the polymer. This decreases the swelling and consequently the pore size of the polymer matrix, which hinders IBU diffusion out of the tablet. Additionally, an increase in the proportion of the grafted copolymer in the matrix tablets increased the IBU release from the matrix tablets. After adding the low amount of MAA grafts (25 mg, F1), swelling and erosion were reduced. CMT-g-MAA copolymer is also present in a protonated state

which accelerates the slower drug release<sup>[50]</sup>. Increasing the graft proportion (up to 175 mg) resulted in higher IBU release due to the repulsion of carboxylate groups causing higher drug release. In basic pH 7.4, the carboxymethyl groups on the CMTKP polymer chains are deprotonated, resulting in a higher negative charge on the polymer. This increases the swelling and subsequently, the pore size of the polymer matrix, allowing for easier diffusion of the drug molecules out of the tablet. Then in the case of CMTKP and CMTKP-g-MAA matrix tablets, the deprotonated carboxylic acid groups on the CMTKP-g-MAA (MAA graft-g-MAA) copolymer and CMTKP can lead to an increase in the swelling and erosion facilitating drug release at pH 7.4. At 6 h, drug release from F1-F6 was 17.85 %, 31.47 %, 36.94 %, 83.62 %, 95.85 % and 25.69 % respectively

( $p < 0.05$ ). Similarly, at 10 h drug release from F1-F6 formulations was significantly different ( $p < 0.05$ ) and was 57.827 %, 90.619 %, 95.631 %, 98.302 %, 100.136 % and 75.117 % in pH 7.4.

The Direct Current (DC) is a measure of the speed at which the drug diffuses in a medium. Increasing the graft polymer in the matrix led to an increase in the DC of IBU. Increasing the graft copolymer amount caused the greater availability of carboxymethyl groups in the bulk. Resulting repulsion of carboxymethyl groups leading to the relaxation of polymeric chains enhanced the DC values (Table 4). The entry of dissolution fluid increased with increasing graft polymer amounts resulting more swelling and drug release.

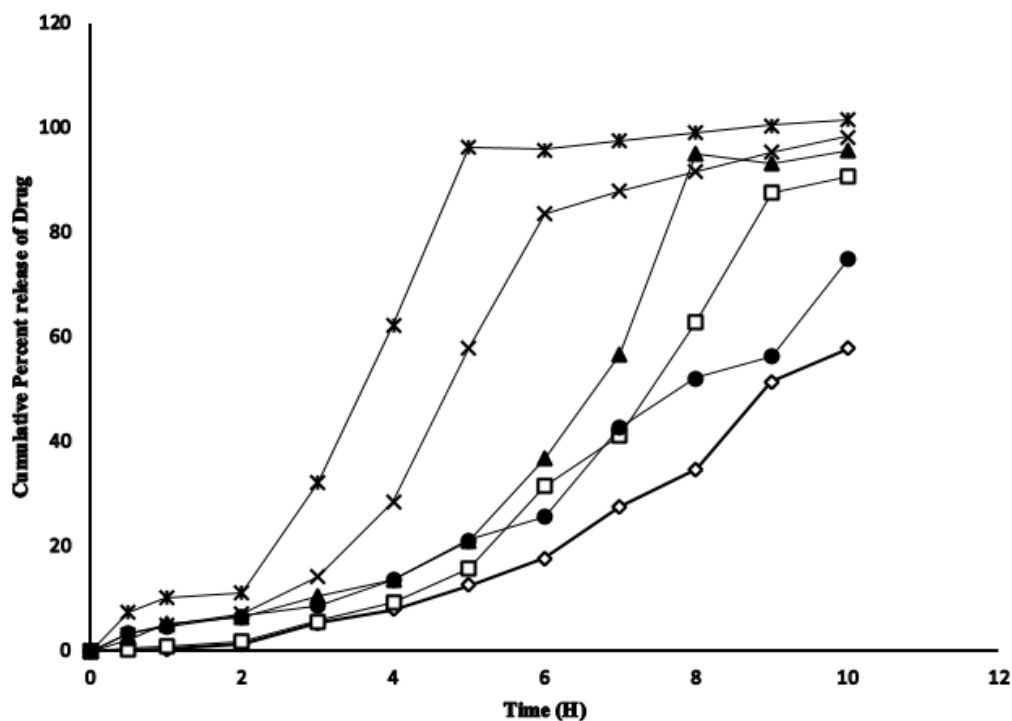


Fig. 12: Drug release study of different formulations in pH 1.2 buffer solution (2 h) followed by pH 7.4 buffer solution to 10 h  
Note: CMTKP/CMTKP-g-MAA: (F1◇): 175:25; (F2□): 150:50; (F3●): 100:100; (F4▲): 50:150; (F5×): 25:175 and (F6\*): 200:0

TABLE 4: DC (D) AND RELEASE EXPONENT (N) OF MATRIX TABLETS

Formulation code	Release exponent (n)	DC (cm <sup>2</sup> /s)
F1	0.45	1.609×10 <sup>-7</sup>
F2	0.507	3.084×10 <sup>-7</sup>
F3	0.763	4.202×10 <sup>-7</sup>
F4	0.787	5.499×10 <sup>-7</sup>
F5	0.819	6.719×10 <sup>-7</sup>
F6	0.853	1.834×10 <sup>-7</sup>

The  $n$  values are shown in Table 4. In the case of the cylindrical matrix such as a tablet, 0.45 indicated Fickian diffusion and  $0.45 < n < 0.89$  indicates anomalous transport. Fickian release stands for diffusion controlled release. Non-Fickian release stands for anomalous release where the drug release may be due to a coupling of Fickian diffusion and polymer relaxation. IBU release from formulation F1 shows Fickian's release ( $n=0.450$ ) i.e., polymer relaxation time was much greater than the characteristics solvent diffusion time. As increased the graft copolymer in the formulations F2, F3, F4 and F5 provide an increment in  $n$  values from 0.507 to 0.819 and shifted to non-Fickian release which denoted the drug release occurs due to a coupling of Fickian diffusion and polymer relaxation<sup>[51]</sup>. The  $n$  value of the only CMTKP matrix tablet (F6) was 0.853, higher than other formulations which also denotes non-Fickian release due to the polymer chain's lower entanglement, rapid drug release and increased DC.

In this study, we reported the grafting of MAA and CMTKP. The grafting was done through the process of free radical polymerization by the conventional method. The reaction was successfully established with optimized grafting parameters (initiator, monomer and polysaccharide concentration, temperature and time of the grafting) to obtain maximized % GE and % G values. The confirmation of grafting was conducted by the FTIR technique. The DSC curve of the IBU drug alone and IBU loaded novel matrix tablet formulation confirmed the thermal stability of the drug. The crystallinity of the IBU was found to be maintained in the prepared tablet formulation with reduced intensities when compared with pure IBU from XRD studies. Swelling, erosion and IBU release were dependent on the pH of the medium. It was less in acidic pH and more in basic pH. Moreover, an increase in the weight ratio of the grafted CMTKP in the matrix tablets increased the swelling, erosion and IBU release from the matrix tablets. The matrix tablets released <8 % of the loaded IBU in the gastric pH and provided sustained IBU release in intestinal pH. We conclude that the developed matrix tablets would bypass the problems associated with IBU administration and thereby enhance patient acceptability and compliance. Further, the characteristics of grafted polymer need to be established. More research is needed to further explore the various drug delivery formulations with the use of this grafted polymer. *In vivo* pharmacokinetics and pharmacodynamics studies will further help to understand the drug delivery options with the grafted polymer.

### Acknowledgments:

The author acknowledges Hindustan Gum, Ltd., for supplying carboxymethyl tamarind kernel powder as a gift sample.

### Authors' contributions:

Conceptualization, data curation, writing-original draft was done by Ankita Das and Kaushik Mukherjee. Writing-review and editing was done by Tapan Kumar Giri.

### Conflict of interest:

The authors declared no conflict of interests.

### REFERENCES

1. Mukherjee K, Dutta P, Badwaik HR, Saha A, Das A, Giri TK. Food industry applications of tara gum and its modified forms. *Food Hydrocoll Health* 2023;3:100107.
2. Buckley C, Murphy EJ, Montgomery TR, Major I. Hyaluronic acid: A review of the drug delivery capabilities of this naturally occurring polysaccharide. *Polymers* 2022;14(17):3442.
3. Giri TK, Verma P, Tripathi DK. Grafting of vinyl monomer onto gellan gum using microwave: Synthesis and characterization of grafted copolymer. *Adv Compos Mater* 2015;24(6):531-43.
4. Grigoras AG. Drug delivery systems using pullulan, a biocompatible polysaccharide produced by fungal fermentation of starch. *Environ Chem Lett* 2019;17(3):1209-23.
5. Shokrani H, Shokrani A, Sajadi SM, Yazdi MK, Seidi F, Jouyandeh M, *et al.* Polysaccharide-based nanocomposites for biomedical applications: A critical review. *Nanoscale Horiz* 2022;7(10):1136-60.
6. Cui M, Zhang M, Liu K. Colon-targeted drug delivery of polysaccharide-based nanocarriers for synergistic treatment of inflammatory bowel disease: A review. *Carbohydr Polym* 2021;272:118530.
7. Giri KT, Thakur A, Tripathi KD. Biodegradable hydrogel bead of casein and modified xanthan gum for controlled delivery of theophylline. *Curr Drug Ther* 2016;11(2):150-62.
8. Mukherjee K, Kundu T, Sa B. Al<sup>3+</sup> ion cross-linked matrix tablets of sodium carboxymethyl cellulose for controlled release of aceclofenac: Development and *in vitro* evaluation. *Der Pharm Lett* 2012;4(6):1633-47.
9. Mukherjee K, Chakraborty S, Sa B. Quick/slow biphasic release of a poorly water soluble antidiabetic drug from bi-layer tablets. *Int J Pharm Pharm Sci* 2015:250-8.
10. Giri TK, Thakur D, Alexander A, Ajazuddin, Badwaik H, Tripathy M, *et al.* Biodegradable IPN hydrogel beads of pectin and grafted alginate for controlled delivery of diclofenac sodium. *J Mater Sci Mater Med* 2013;24(5):1179-90.
11. Mukherjee K, Dutta P, Giri TK. Al<sup>3+</sup>/Ca<sup>2+</sup> cross-linked hydrogel matrix tablet of etherified tara gum for sustained delivery of tramadol hydrochloride in gastrointestinal milieu. *Int J Biol Macromol* 2023;232:123448.
12. Dey M, Ghosh B, Giri TK. Enhanced intestinal stability and

- pH sensitive release of quercetin in GIT through gellan gum hydrogels. *Colloids Surf B Biointerfaces* 2020;196:111341.
13. Giri TK, Dey B, Maity S. Preparation and characterization of nanoemulsome entrapped in enteric coated hydrogel beads for the controlled delivery of capsaicin to the colon. *Curr Drug Ther* 2018;13(1):98-105.
  14. Vu VV, Beeson WT, Phillips CM, Cate JH, Marletta MA. Determinants of regioselective hydroxylation in the fungal polysaccharide monooxygenases. *J Am Chem Soc* 2014;136(2):562-5.
  15. Kaur H, Yadav S, Ahuja M, Dilbaghi N. Synthesis, characterization and evaluation of thiolated tamarind seed polysaccharide as a mucoadhesive polymer. *Carbohydr Polym* 2012;90(4):1543-9.
  16. Seidi F, Salimi H, Shamsabadi AA, Shabani M. Synthesis of hybrid materials using graft copolymerization on non-cellulosic polysaccharides *via* homogenous ATRP. *Prog Polym Sci* 2018;76:1-39.
  17. Kang H, Liu R, Huang Y. Graft modification of cellulose: Methods, properties and applications. *Polymer* 2015;70:A1-6.
  18. Shukla A, Maity S, Ray B, Maiti P. Dextrin and polyurethane graft copolymers as drug carrier: Synthesis, characterization, drug release, biocompatibility and *in vitro* toxicity. *Carbohydrate Polym Technol Appl* 2021;2:100171.
  19. Li MC, Lee JK, Cho UR. Synthesis, characterization, and enzymatic degradation of starch-grafted poly (methyl methacrylate) copolymer films. *J Appl Polym Sci* 2012;125(1):405-14.
  20. Savin CL, Popa M, Delaite C, Costuleanu M, Costin D, Peptu CA. Chitosan grafted-poly (ethylene glycol) methacrylate nanoparticles as carrier for controlled release of bevacizumab. *Mater Sci Eng C Mater Biol Appl* 2019;98:843-60.
  21. Shahid M, Bukhari SA, Gul Y, Munir H, Anjum F, Zuber M, *et al.* Graft polymerization of guar gum with acryl amide irradiated by microwaves for colonic drug delivery. *Int J Biol Macromol* 2013;62:172-9.
  22. Dheer D, Arora D, Jaglan S, Rawal RK, Shankar R. Polysaccharides based nanomaterials for targeted anti-cancer drug delivery. *J Drug Target* 2017;25(1):1-6.
  23. Kalia S, Saba MW. Polysaccharide based graft copolymers. 1<sup>st</sup> ed. Heidelberg (New York): Springer Publishers; 2013.
  24. Mendoza DJ, Ayurini M, Browne C, Raghuvanshi VS, Simon GP, Hooper JF, *et al.* Thermoresponsive poly (n-isopropylacrylamide) grafted from cellulose nanofibers *via* silver-promoted decarboxylative radical polymerization. *Biomacromolecules* 2022;23(4):1610-21.
  25. Tripathi R, Mishra B. Development and evaluation of sodium alginate-polyacrylamide graft-co-polymer-based stomach targeted hydrogels of famotidine. *Aaps Pharmscitech* 2012;13:1091-102.
  26. Povea MB, Monal WA, Cauich-Rodríguez JV, Pat AM, Rivero NB, Covas CP. Interpenetrated chitosan-poly (acrylic acid-co-acrylamide) hydrogels. Synthesis, characterization and sustained protein release studies. *Mater Sci Appl* 2011;2(06):509.
  27. Pal S, Ghorai S, Dash MK, Ghosh S, Udayabhanu G. Flocculation properties of polyacrylamide grafted carboxymethyl guar gum (CMG-g-PAM) synthesised by conventional and microwave assisted method. *J Hazardous Mater* 2011;192(3):1580-8.
  28. Bushra R, Aslam N. An overview of clinical pharmacology of ibuprofen. *Oman Med J* 2010;25(3):155.
  29. Sun T, Xu P, Liu Q, Xue J, Xie W. Graft copolymerization of methacrylic acid onto carboxymethyl chitosan. *Eur Polym J* 2003;39(1):189-92.
  30. Agnihotri SA, Aminabhavi TM. Controlled release of clozapine through chitosan micro particles prepared by a novel method. *J Control Release* 2004;96(2):245-59.
  31. Ritger PL, Peppas NA. A simple equation for description of solute release II. Fickian and anomalous release from swellable devices. *J Control Release* 1987;5(1):37-42.
  32. Yoshida T, Hattori K, Sawada Y, Choi Y, Uryu T. Graft copolymerization of methyl methacrylate onto curdlan. *J Polymer Sci Part A* 1996;34(15):3053-60.
  33. Mali KK, Dhawale SC, Dias RJ. Synthesis and characterization of hydrogel films of carboxymethyl tamarind gum using citric acid. *Int J Biol Macromol* 2017;105:463-70.
  34. Warkar SG, Kumar A. Synthesis and assessment of carboxymethyl tamarind kernel gum based novel superabsorbent hydrogels for agricultural applications. *Polymer* 2019;182:121823.
  35. Pandit AP, Waychal PD, Sayare AS, Patole VC. Carboxymethyl tamarind seed kernel polysaccharide formulated into pellets to target at colon. *Indian J Pharm Educ Res* 2018;52:363-73.
  36. Garcia DM, Escobar JL, Bada N, Casquero J, Hernández E, Katime I. Synthesis and characterization of poly (methacrylic acid) hydrogels for metoclopramide delivery. *Eur Polymer J* 2004;40(8):1637-43.
  37. Abbasian M, Roudi MM, Mahmoodzadeh F, Eskandani M, Jaymand M. Chitosan-grafted-poly (methacrylic acid)/ graphene oxide nanocomposite as a pH-responsive *de novo* cancer chemotherapy nanosystem. *Int J Biol Macromol* 2018;118:1871-9.
  38. Mundargi RC, Agnihotri SA, Patil SA, Aminabhavi TM. Graft copolymerization of methacrylic acid onto guar gum, using potassium persulfate as an initiator. *J Appl Polym Sci* 2006;101(1):618-23.
  39. Behari K, Pandey PK, Kumar R, Taunk K. Graft copolymerization of acrylamide onto xanthan gum. *Carbohydr Polym* 2001;46(2):185-9.
  40. Hsu SC, Don TM, Chiu WY. Free radical degradation of chitosan with potassium persulfate. *Polym Degrad Stab* 2002;75(1):73-83.
  41. Hosseinzadeh H. Ceric-initiated free radical graft copolymerization of acrylonitrile onto kappa carrageenan. *J Appl Polym Sci* 2009;114(1):404-12.
  42. Tiwari A, Singh V. Microwave-induced synthesis of electrical conducting gum acacia-graft-polyaniline. *Carbohydrate Polym* 2008;74(3):427-34.
  43. Kumar D, Mundlia J, Kumar T, Ahuja M. Silica coating of carboxymethyl tamarind kernel polysaccharide beads to modify the release characteristics. *Int J Biol Macromol* 2020;146:1040-9.
  44. Tița B, Fuliș A, Szabadai Z, Rusu G, Bandur G, Tița D. Compatibility study between ibuprofen and excipients in their physical mixtures. *J Thermal Anal Calorim* 2011;105(2):517-27.
  45. Pal S, Sen G, Mishra S, Dey RK, Jha U. Carboxymethyl tamarind: Synthesis, characterization and its application as novel drug-delivery agent. *J Appl Polym Sci* 2008;110(1):392-400.

46. Guler MA, Gok MK, Figen AK, Ozgumus S. Swelling, mechanical and mucoadhesion properties of Mt/starch-g-PMAA nanocomposite hydrogels. *Appl Clay Sci* 2015;112:44-52.
  47. Ghaffar AM, El-Arnaouty MB, Baky AA, Shama SA. Radiation-induced grafting of acrylamide and methacrylic acid individually onto carboxymethyl cellulose for removal of hazardous water pollutants. *Des Monomers Polym* 2016;19(8):706-18.
  48. Uhrich KE, Cannizzaro SM, Langer RS, Shakesheff KM. Polymeric systems for controlled drug release. *Chem Rev* 1999;99(11):3181-98.
  49. Pillai O, Panchagnula R. Polymers in drug delivery. *Curr Opin Chem Biol* 2001;5(4):447-51.
  50. Patel NK, Joshi J, Mishra D, Patel VA, Sinha VK. Controlled release of carbamazepine from carboxymethyl chitosan-grafted-2-hydroxyethylmethacrylate matrix tablets. *J Appl Polym Sci* 2010;115(6):3442-50.
  51. Kulkarni RV, Baraskar VV, Alange VV, Naikawadi AA, Sa B. Controlled release of an antihypertensive drug through interpenetrating polymer network hydrogel tablets of tamarind seed polysaccharide and sodium alginate. *J Macromol Sci B* 2013;52(11):1636-50.
-